Final Draft
of the original manuscript:

Tung, W.; Zou, J.; Sun, X.; Wang, W.; Gould, O.; Kratz, K.; Ma, N.; Lendlein, A.:

Coaxial electrospinning of PEEU/gelatin to fiber meshes with enhanced mesenchymal stem cell attachment and proliferation

In: Clinical Hemorheology and Microcirculation. Vol. 74 (1) 2020. 53 - 66.
First published online by IOS: February 22, 2020

DOI: 10.3233/CH-199235
https://dx.doi.org/10.3233/CH-199235

Co-axial electrospinning of PEEU/Gelatin to fiber meshes with enhanced mesenchymal stem cell attachment and proliferation

Wing Tai Tung[1,2], Jie Zou[1], Xianlei Sun[1,2], Weiwei Wang[1], Oliver E. C. Gould[1], Karl Kratz[1], Nan Ma[1,3]*, Andreas Lendlein[1,2,3]*

[1] Institute of Biomaterial Science and Berlin-Brandenburg Centre for Regenerative Therapies, Helmholtz-Zentrum Geesthacht, Kantstrasse 55, 14513 Teltow, Germany

[2] University of Potsdam, Karl-Liebknecht-Str. 24/25, 14476 Potsdam, Germany

[3] Institute of Chemistry and Biochemistry, Freie Universität Berlin, 14195 Berlin, Germany

Abstract

Microfibers with a core-shell structure can be produced by co-axial electrospinning, allowing for the functionalization of the outer layer with bioactive molecules. In this study, a thermoplastic, degradable polyesteretherurethane (PEEU), consisting of poly(p-dioxanone) (PPDO) and poly(ε-caprolactone) (PCL) segments with different PPDO to PCL weight ratios, were processed into fiber meshes by co-axial electrospinning with gelatin. The prepared PEEU fibers have a diameter of 1.3 ± 0.5 µm and an elastic modulus of around 5.1 ± 1.0 MPa as measured by tensile testing in a dry state at 37 °C, while the PEEU/Gelatin core-shell fibers with a gelatin content of 12 ± 6 wt% and a diameter of 1.5 ± 0.5 µm possess an elastic modulus of 15.0 ± 1.1 MPa in a dry state at 37 °C but as low as 0.7 ± 0.7 MPa when hydrated at 37 °C. Co-axial electrospinning allowed for the homogeneous distribution of the gelatin shell along the whole microfiber. Gelatin with conjugated fluorescein (FITC) remained stable on the PEEU fibers after 7 days incubation in phosphate-buffered saline (PBS) at 37 °C. The gelatin coating on PEEU fibers lead to enhanced human adipose tissue derived mesenchymal stem cell (hADSC) attachment and a proliferation rate 81.7 ± 34.1 % higher in cell number in PEEU50/Gelatin fibers after 7 days of cell culture when compared to PEEU fibers without coating. In this work, we demonstrate that water-soluble gelatin can be incorporated as the outer shell of a polymer fiber via molecular entanglement, with a sustained presence and role in enhancing stem cell attachment and proliferation.

Keywords: PEEU, gelatin, electrospun fibers, mesenchymal stem cells, biomaterials,

Introduction

Tailoring the structure and architecture of a specific material is important in ensuring its successful function in a particular application, for example as a hydrogel scaffold, drug delivery vector [1–3], patch in wound healing [4,5], or biomedical implant for tissue replacement [6–8]. Electrospinning has become prevalent as a technique to produce micro/nanofibers at comparable length scales to the native extracellular matrix (ECM) [9], providing a method to transform polymers into functional fiber structures and fiber mesh architectures [10–13].

The mechanical properties of a micro/nanofiber mesh differ greatly from a bulk material film. The highly intersected and suspended nature of micro/nanofibers in a fiber mesh causes a significant variation in local elastic properties [14] , which the cells interpret through integrin and focal adhesion as they interact with the fibers, transmitting the mechanical signal intracellularly via the cytoskeleton [15]. The high surface to volume or mass ratio of electrospun fibers enables more effective interaction between the bioactive molecules and the cells [16], as compared to film-based substrates [17,18]. This interaction activates cellular signaling through integrin and ligand interaction, regulating cellular functionality, and modifying cell attachment and proliferation [19,20].

The deposition of a homogeneous polymer shell onto a polymer core has been demonstrated using co-axial electrospinning [21,22]. To achieve this, a smaller diameter blunt needle is installed inside of a larger diameter blunt needle [23]. This method completely isolates the two components until ejection from the co-axial needle and solvent evaporation, leaving solidified core-shell micro/nanofibers on the collector. Previous work has demonstrated core-shell fibers, used for sustainable delivery, where bioactive molecules are used as the core material [24,25]. Biomolecules have also been integrated on the surface of a polymeric core via co-axial electrospinning to enhance cellular functionality [26,27].

Gelatin denatured from collagen is a commonly used biopolymer. Gelatin is soluble in water and requires crosslinking, such as with glutaraldehyde [26–28] or genipin [29], to produce stable fibers in an aqueous environment. However, the toxicity of glutaraldehyde makes it undesirable in biological environments, and any crosslinking procedure can disrupt the fiber scaffold architecture [30]. Here, we hypothesise that

by co-axial electrospinning gelatin as a shell layer, we can use the same solvent for both components, forming a polymer-enforced bioactive gelatin cover on core-shell fibers. The generated homogenous gelatin layer deposited on the core polymer should enhance cellular functionality, such as cell attachment and proliferation. The polymer used in this study is polyesteretherurethane (PEEU), a multiblock copolymer containing poly(*ε*-caprolactone) (PCL) and poly(*p*-dioxanone) (PPDO) segments (Fig. 1) with angiogenesis potential [31]. PEEU polymers with different PPDO to PCL ratios were electrospun into fibers via traditional electrospinning and PEEU/Gelatin fibers via co-axial electrospinning. The mechanical and thermal properties of the fibers were characterized to correlate their composition dependence. Human adipose derived stem cells (hADSCs) were cultured on the fiber meshes to investigate the effect of the PEEU fiber composition and the gelatin shell on cell attachment and proliferation. In this work a method for the preparation of biochemically functionalized fiber meshes is shown, and the potential of core/shell fibrous scaffolds in the culture of human adipose derived stem cells is demonstrated.

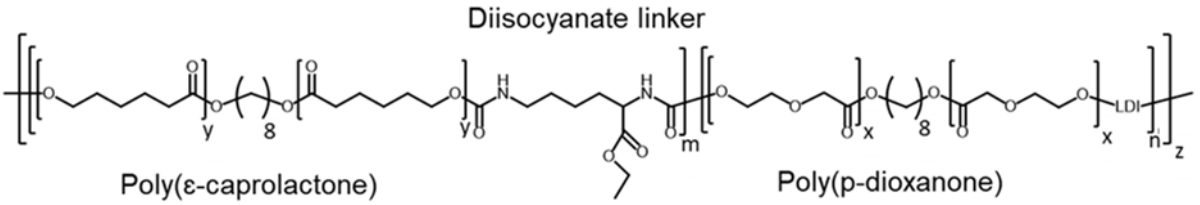

Figure 1. Chemical structure of PEEU. Molecular formula of polyesteretherurethane (PEEU) copolymer.

Materials and Methods

Chemical and reagents

The polyesteretherurethane (PEEU) copolymers composed of PPDO and PCL with four different PPDO:PCL ratios (Table 1) were obtained as described previously [32]. Gelatin powder (bloom strength of 215 - 235 g) was purchased from Rousselot (Gustav Parmentier GmbH, 60320 Frankfurt am Main, Germany). Hexafluoro-isopropanol (HFIP) was used for dissolving the polymer and gelatin into solution for electrospinning, which was purchased from abcr GmbH (AB102635) (abcr GmbH, 76187 Karlsruhe, Germany). Cell culture medium (DMEM+GlutaMAX-I) used for human adipose tissue derived mesenchymal stem cells (hADSCs) was purchased from Fisher Scientific GmbH (31966-021) (58239 Schwerte, Germany). The Fetal Bovine Serum (FBS, F7524) was obtained from Sigma-Aldrich (Darmstadt, Germany).

Table 1. PEEU material information

Material ID	PPDO : PCL wt ratio	Molecular weight (Mw) (g/mol)	Solution conc. for electrospinning (wt%)
PEEU40	40 : 60	100,000	14
PEEU50	50 : 50	79,000	17
PEEU60	60 : 40	95,000	15
PEEU70	70 : 30	133,000	11

Preparation of electrospun fibers

The electrospinning setup (Linari Engineering, 56121 Pisa, Italy) included voltage supply, rotatory drum collector and two syringe pumps. The electrospinning process was performed inside a transparent plastic chamber connected with a variable air supply for humidity control. The PEEU polymers were dissolved in HFIP at the concentrations listed in Table 1. The gelatin was dissolved in HFIP at 3 wt%. All solutions were filtered with a glass fiber syringe filter with a pore size of 1 μm before electrospinning. For PEEU fiber electrospinning, a gauge 19 blunt tip needle was used. For co-axial electrospinning, the co-axial needle module (Linari Engineering) was used where the inner blunt tip needle was gauge 21 and the outer was gauge 15. The distance from the needle tip to the collector was set at 25 cm. The flowrate of solution supply during electrospinning was 1.77 mL/h for pure PEEU electrospinning, and 1.13 mL/h and 0.57 ml/h for core PEEU solution and shell gelatin solution, respectively during co-axial electrospinning. A polypropylene film was wrapped over the rotatory

drum collector for collecting deposited fiber mesh. The drum collector was rotated at 5 rpm, a humidity of 20% and an applied voltage of 10-18 kV was maintained and raised during the course of electrospinning.

Scanning electron microscopy (SEM)

The morphology of fiber meshes was characterized using scanning electron microscopy (Phenom G2 Pro, Phenom World). The samples were first incubated in vacuum overnight and coated with 5 nm gold in sputter coater (Polaron SC7640). The samples were then transferred to the sample holder of the SEM. SEM was used to determine fiber diameter.

Differential scanning calorimetry (DSC)

Thermal properties of the PEEU fibers were obtained using DSC (Netzsch DSC 204 Phoenix, NETZSCH-Gerätebau GmbH, Selb, Germany) under nitrogen gas flow. 5 mg of each sample was weighed into an aluminum pan and sealed. The heating, cooling and second heating were performed from 25 ^{o}C to 150 ^{o}C, 150 ^{o}C to -100 ^{o}C, and -100 ^{o}C to 150 ^{o}C, respectively at a rate of 10 K/min, with a 2 min holding stage at upper and lower end point temperature. An empty aluminum pan was used as reference.

Thermogravimetric analysis (TGA)

The thermogravimetric analysis was performed using Netzsch TG 209 C Iris (NETZSCH-Gerätebau GmbH, Selb, Germany). The fibers samples (5 mg) were heated from 25 ^{o}C to 600 ^{o}C at a rate of 10 K/min under a nitrogen gas atmosphere. The weight loss of the samples during the heating was recorded.

Porosities and gelatin content

Porosities of all the PEEU and PEEU/Gelatin fibers meshes were calculated from the mass of the fiber mesh and the corresponding volume, together with the corresponding density value. The gelatin content was calculated from the remained percentage mass

of bulk gelatin, PEEU fibers and PEEU/Gelatin fibers in TGA using the following equation

$$Gelatin\ content = \frac{PEEU/Gelatin\ wt\% - PEEU\ wt\%}{Gelatin\ wt\% - PEEU\ wt\%}.$$

Tensile test

The tensile test of fiber samples was performed inside the temperature chamber of tensile test apparatus (Zwick GmbH, Ulm, Germany) at 37 ºC in a dry state. The fiber samples were cut into 1 cm x 4 cm strips. Each sample was clamped inside the temperature chamber before equilibration at 37 ºC before measurement. For tensile testing in water, the measurement was performed on a tensile test machine with water tank (Zwick GmbH, Ulm, Germany) at 37 ºC. Test samples were hydrated in the water tank for 10 minutes before the start of measurement.

Fiber samples pre-treatment before cell culture

The PEEU and PEEU/Gelatin fiber meshes were first packed in sterilization bags followed with sterilization under ethylene oxide at 45 ºC for 3 hours. The fiber meshes were then punched into a circular shaped sample with 1.2 mm in diameter. PEEU fiber meshes were washed overnight before cell culture.

FITC conjugation on PEEU/Gelatin fiber meshes

The PEEU/Gelatin core-shell fiber samples for immunostaining were conjugated with NHS-FITC (46410, Thermo Fisher Scientific). 10 mg NHS-FITC was dissolved in 100 µl DMSO and transferred into 10 ml pH8 sodium carbonate buffer. The NHS-FITC in sodium carbonate buffer was filtered with sterile 0.2 µm pore size syringe filter. The PEEU/Gelatin fibers were conjugated with the NHS-FITC in pH 8 sodium carbonate buffer for 1.5 h followed by washing with PBS overnight. The FITC conjugated PEEU/Gelatin fibers were incubated in PBS at 37 ºC over 7 days to demonstrate the retention of gelatin on fibers in aqueous environment. The PBS was changed as the cell culture medium changed, i.e. on day 2, 4 and 6, to ensure the FITC conjugated PEEU/Gelatin fibers experience comparable condition as the PEEU/Gelatin fibers used in cell culture.

Cell culture

Human adipose derived mesenchymal stem cells (hADSCs) were cultured in Dulbecco's Modified Eagle Medium (DMEM+GlutaMAX) with 10 v/v% FBS, 100 I.U./mL penicillin and 100 µg/ml streptomycin. hADSC was seeded at 1 x 10^4 cells per fiber sample in each well of 24 well-plate (ultra-low attachment). Cell proliferation was tested using a cell counting kit (CCK8, Dojindo) according to the protocol supplied by manufacturer. Briefly, at selected time points, the medium was replaced with 300 µl of fresh medium followed by the addition of 30 ul of CCK8 solution. After 2 hours of incubation at 37 ^oC, 100 µl of medium/CCK8 mixture from each sample was transferred into a flat bottom 96 well plate. An absorbance at wavelength of 450 nm was measured using a microplate reader (Infinite 200 Pro, Tecan Group Ltd., Mannedorf, Switzerland). A standard curve, generated from the absorbance of a series of cells with known cell numbers, was used in the calculation of cell numbers on the fiber meshes.

Immunostaining

The hADSCs on PEEU and PEEU/Gelatin fiber meshes were fixed with 4 wt% PFA. After washing with PBS for 3 times, the cells were permeabilized with 0.1 v/v% triton x-100 for 15 minutes, followed by washing with PBS for 3 times again. The cells were incubated in the blocking buffer (2 wt% bovine serum albumin in PBS) for 1 h to block non-specific antigen. ActinRed (R37112, Invitrogen) was used for staining actin, and NucBlue (R37605, Invitrogen) for nucleus of hADSC.

Statistics

The number of repetitions for each experiment was larger than three, as indicated respectively in the figure legends for each assay, with data expressed as a mean value ± standard deviation. Statistical analysis was performed using a two-tailed independent sample *t*-test, and a significance level *p* value less than 0.05 was considered to be statistically significant.

Results and Discussion

Fiber morphology and fiber diameter

The morphology of the fiber meshes was examined using SEM (Fig. 2a). The PEEU fibers possessed a circular cylinder shape and smooth surface. In contrast, the PEEU/Gelatins fibers showed a flattened morphology due to the fast evaporation of the outer gelatin shell layer [33], resulting in a hardened surface layer where the inner PEEU accumulated on the inner side of the shell during the evaporation of inner HFIP. This hollow structure led to the fiber's collapse forming a flattened morphology [34]. The diameter of PEEU fibers (Fig. 2b) displayed a dependency on polymer weight average molecular weight (Table 1). The PEEU50 had the lowest molecular weight and smallest fiber diameter (Fig. 2b), despite having the highest electrospinning solution concentration. Concentrations used throughout, described in the methods section, were chosen to avoid artifact bead formation during electrospinning. The PEEU70 with the highest molecular weight (Table 1) resulted in the largest fiber diameter in the PEEU group (Fig. 2b). In the PEEU/Gelatin group, the lowest PEEU molecular weight PEEU50/Gelatin fiber also had the smallest fiber diameter while the PEEU60/Gelatin and PEEU70/Gelatin fibers displayed higher diameters (Fig. 2b). The largest diameter of PEEU60/Gelatin fibers was observed in the fibers with the lowest gelatin content, i.e. highest PEEU content, in the fiber mesh (Table 2).

Table 2. Porosities and gelatin content of fiber meshes

Material ID	Porosity (%)	Gelatin Content (wt%)
PEEU40	62.3 ± 0.5	-
PEEU50	62.8 ± 0.9	-
PEEU60	62.0 ± 1.5	-
PEEU70	63.4 ± 1.0	-
PEEU40Gt	61.9 ± 0.7	11 ± 0.1
PEEU50Gt	65.7 ± 0.8	13 ± 0.1
PEEU60Gt	65.2 ± 1.7	5 ± 0.1
PEEU70Gt	66.3 ± 1.7	12 ± 0.1

Gt: gelatin

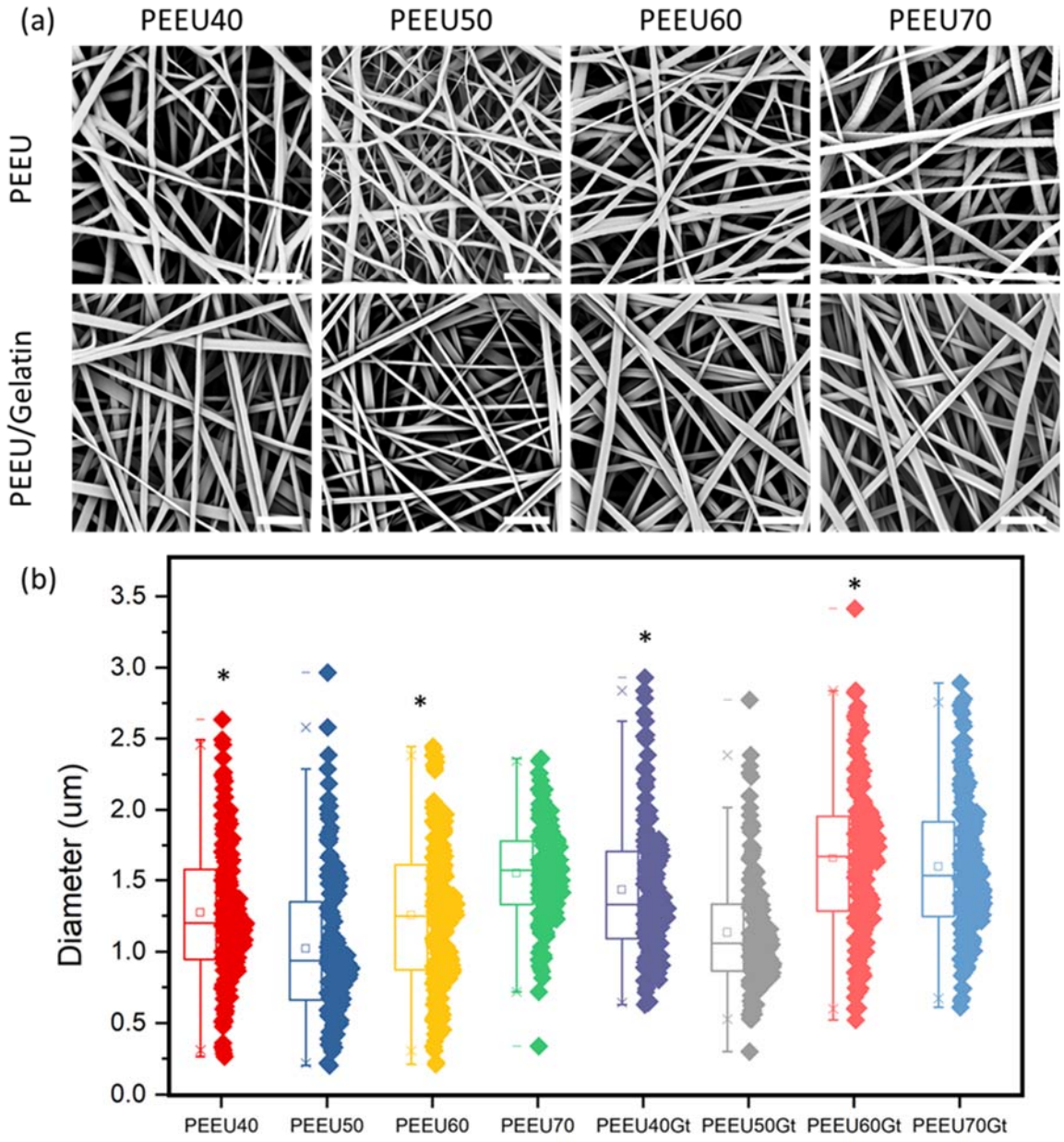

Figure 2. Morphology and fiber diameter distribution of PEEU and PEEU/Gelatin fiber meshes. (a) SEM images of the PEEU and PEEU/Gelatin fiber meshes. Scale bar = 10 μm. (b) The diameters of PEEU and PEEU/Gelatin fibers in box and dot plot. Gt: gelatin. □ = mean, x = 1% and 99% percentile, - = max or min. (n > 150). *: significant difference between the PEEU and its corresponding PEEU with gelatin shell, p < 0.05.

Porosity and gelatin content

The fiber mesh displayed similar porosities (Table 2) for all of the materials used. The obtained values of approximately 60% suggest that the spaces to accommodate cells within the fiber meshes are similar for all materials used. The gelatin contents of the PEEU/Gelatin fibers displayed a comparable amount, i.e. 12 wt%, among the samples examined (Table 2), with an exception of PEEU60/Gelatin which displayed the lowest

at 5 wt%. All PEEU/Gelatin fiber samples were electrospun under the similar conditions, with only a variation in polymer solution concentration, which was kept the same as for the pure PEEU samples.

Mechanical properties of PEEU and PEEU/Gelatin fibers

The elastic modulus of the PEEU fibers at 37 °C in the dry state (Table 3) increased with the weight percentage of PPDO, while the elongation of break and maximum stress (Table 3 and Fig. 3.) correlated with molecular weight (Fig. 1). For the PEEU/Gelatin fibers, the elastic moduli were observed to be higher than those of PEEU fibers (Table 3), suggesting that the gelatin shell reinforced the polymer fibers in the dry state. This finding was consistent with previous studies, in which fiber reinforcement by the incorporation of gelatin during electrospinning has been reported [30,35–36]. Elastic moduli were found to be similar among PEEU40/Gelatin, PEEU50/Gelatin and PEEU60/Gelatin, which gave lower values than those of PEEU70/Gelatin. This suggests that the variation of PPDO to PCL weight ratio had no effect on the elastic moduli of the core/shell fibers prepared by co-axial electrospinning. However, a variation in elongation of break and maximum stress values of the PEEU/Gelatin fiber meshes with PEEU weight average molecular weight was observed (Table 3 and Fig. 3). The PEEU50 with the lowest molecular weight displayed the lowest elongation of break of a PEEU50/Gelatin fiber mesh.

Table 3. Mechanical properties of dry PEEU and PEEU/Gelatin fibers at 37ºC

Material ID	Elastic modulus (MPa)	Elongation at break (%)	Maximum stress (MPa)
PEEU40	4.1 ± 0.3	228 ± 50	1.3 ± 0.2
PEEU50	5.2 ± 0.4	123 ± 22	1.1 ± 0.1
PEEU60	4.7 ± 0.4	252 ± 17	1.6 ± 0.1
PEEU70	6.5 ± 0.6	266 ± 47	2.1 ± 0.1
PEEU40Gt	14.3 ± 1.0	110 ± 8	1.6 ± 0.1
PEEU50Gt	15.0 ± 0.7	8 ± 1	1.2 ± 0.1
PEEU60Gt	14.1 ± 0.9	191 ± 14	1.9 ± 0.2
PEEU70Gt	16.4 ± 2.6	194 ± 45	2.6 ± 0.3

Gt: gelatin

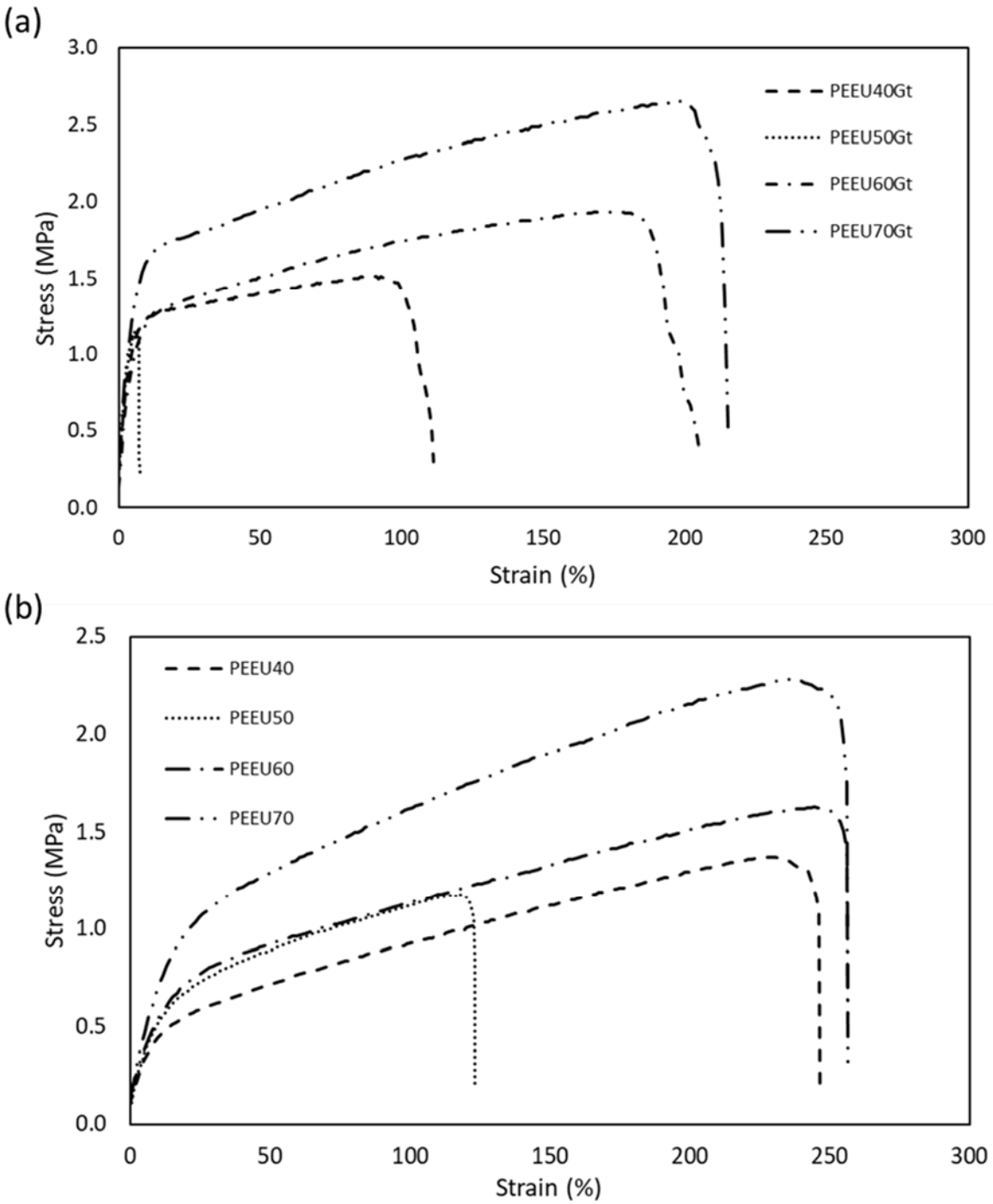

Figure 3. Stress-strain curves of dry PEEU and PEEU/Gelatin fibers at 37 ºC. (Gt: gelatin)

The hydration of PEEU/Gelatin fibers in water at 37 ºC altered their mechanical properties. Data obtained during the mechanical characterization of the samples is summarized in Table. 4. In the dry state, a high elastic moduli PEEU/Gelatin was measured (Table 3). When the PEEU/Gelatin fiber meshes were hydrated in water, the elastic moduli were reduced to below 1.6 MPa (Table 4). The elastic modulus

enforcement in PEEU/Gelatin core shell fibers in dry state was a result of the glassy state of the gelatin shell. In the presence of water, the lowering of the glass transition temperature of the gelatin shell led to it becoming amorphous, and subsequently unable to provide mechanical strength against the applied force.

The elongation at break of PEEU/Gelatin fiber meshes displayed a dependency on gelatin content. Samples with a gelatin content of above 10 wt% (Table 2), showed values for elongation at break of above 500% while PEEU60/Gelatin samples with a gelatin content of 5 wt% gave values of 270 ± 59% for the elongation at break (Table 4). The maximum stress of PEEU/Gelatin fiber meshes depended on the material used for the polymer core, where the PEEU60/Gelatin samples, with 95% PEEU60 content, had the highest maximum stress (Table 2).

Table 4. Mechanical properties of PEEU/Gelatin fibers at 37ºC in water

Material ID	Elastic modulus (MPa)	Elongation at break (%)	Maximum stress (MPa)
PEEU40Gt	0.1 ± 0.0	512 ± 42	0.7 ± 0.1
PEEU50Gt	0.2 ± 0.1	518 ± 14	0.5 ± 0.0
PEEU60Gt	1.6 ± 0.2	270 ± 59	2.8 ± 0.2
PEEU70Gt	0.8 ± 0.1	512 ± 24	0.6 ± 0.0

Thermal properties

DSC curves of PEEU40 and PEEU40/Gelatin fibers are shown in Fig. 4a and Fig. 4b, respectively as representative curves of the PEEU and PEEU/Gelatin fibers group. The thermal properties, listed in Table 5, were derived from the second heating curve. The enthalpy values measured for PCL crystallinity were similar in samples with and without gelatin, but enthalpy values measured for the PPDO crystallinity were reduced in the PEEU/Gelatin group when compared to the PEEU group. This suggested that the presence of gelatin had an effect on the crystallinity of PPDO. This is in agreement with the observed reduction in mechanical strength of the PEEU/Gelatin fibers in water.

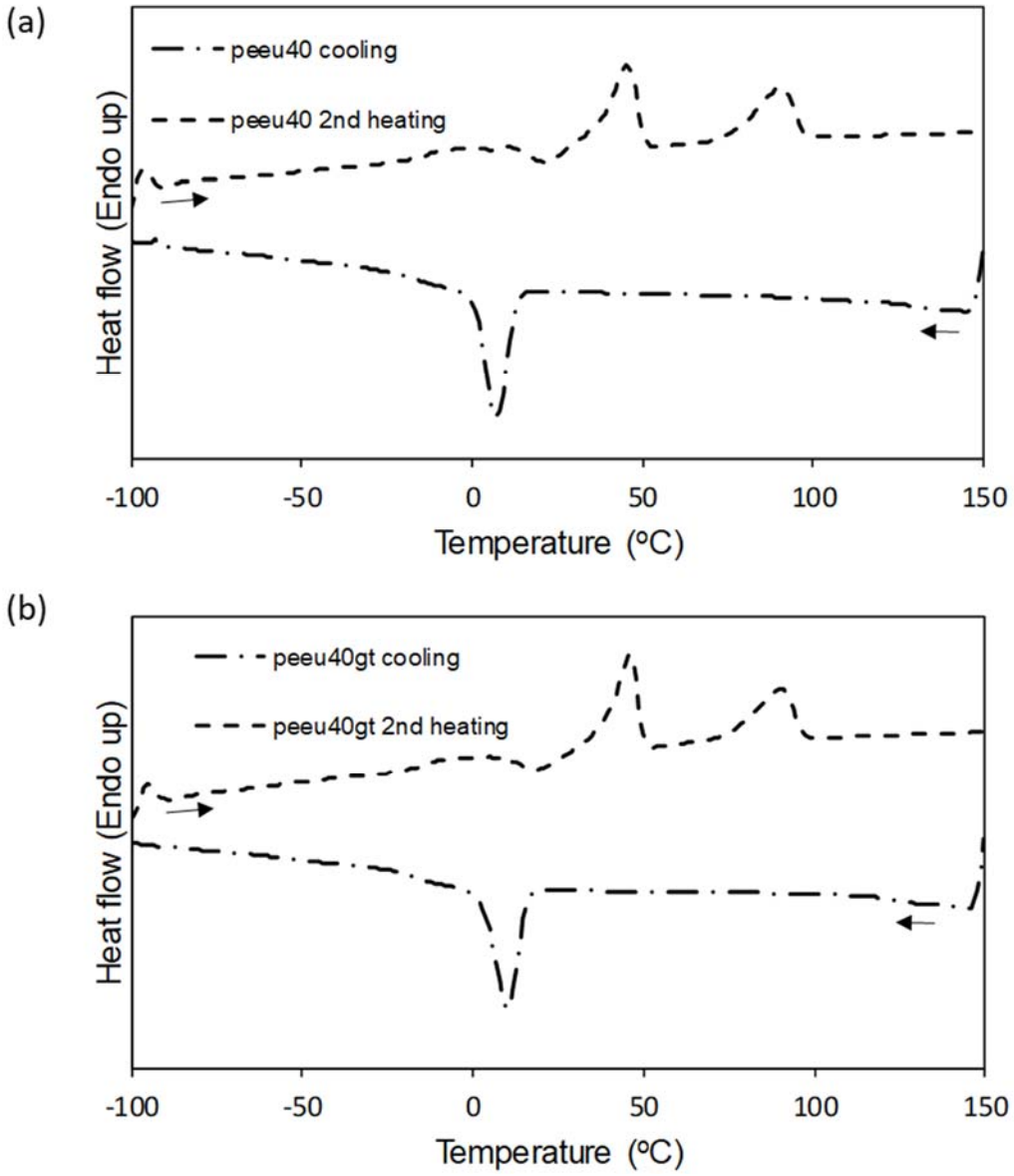

Figure 4. DSC curves of PEEU and PEEU/Gelatin fibers. (a) DSC curves of PEEU40 fibers. (b) DSC curves of PEEU40/Gelatin fibers.

Table 5. Thermal properties of PEEU and PEEU/Gelatin

Material ID	$T_{m,PCL}$ (°C)	En_{PCL} (J/g)	$T_{m,PPDO}$ (°C)	En_{PPDO} (J/g)
PEEU40	45.5 ± 0.5	22.7 ± 0.2	90.5 ± 0.9	19.7 ± 0.2
PEEU50	44.7 ± 0.4	19.1 ± 0.2	92.3 ± 0.9	27.2 ± 0.3
PEEU60	43.8 ± 0.4	17.5 ± 0.2	95.3 ± 1.0	35.0 ± 0.4
PEEU70	39.5 ± 0.4	4.6 ± 0.1	92.5 ± 0.9	33.6 ± 0.3
PEEU40Gt	46.1 ± 0.4	19.3 ± 0.2	90.1 ± 0.9	16.1 ± 0.2
PEEU50Gt	44.2 ± 0.4	17.8 ± 0.2	92.3 ± 0.9	24.5 ± 0.2
PEEU60Gt	43.1 ± 0.4	13.3 ± 0.1	95.2 ± 1.0	28.7 ± 0.3
PEEU70Gt	39.1 ± 0.4	4.4 ± 0.1	91.8 ± 0.9	28.9 ± 0.3

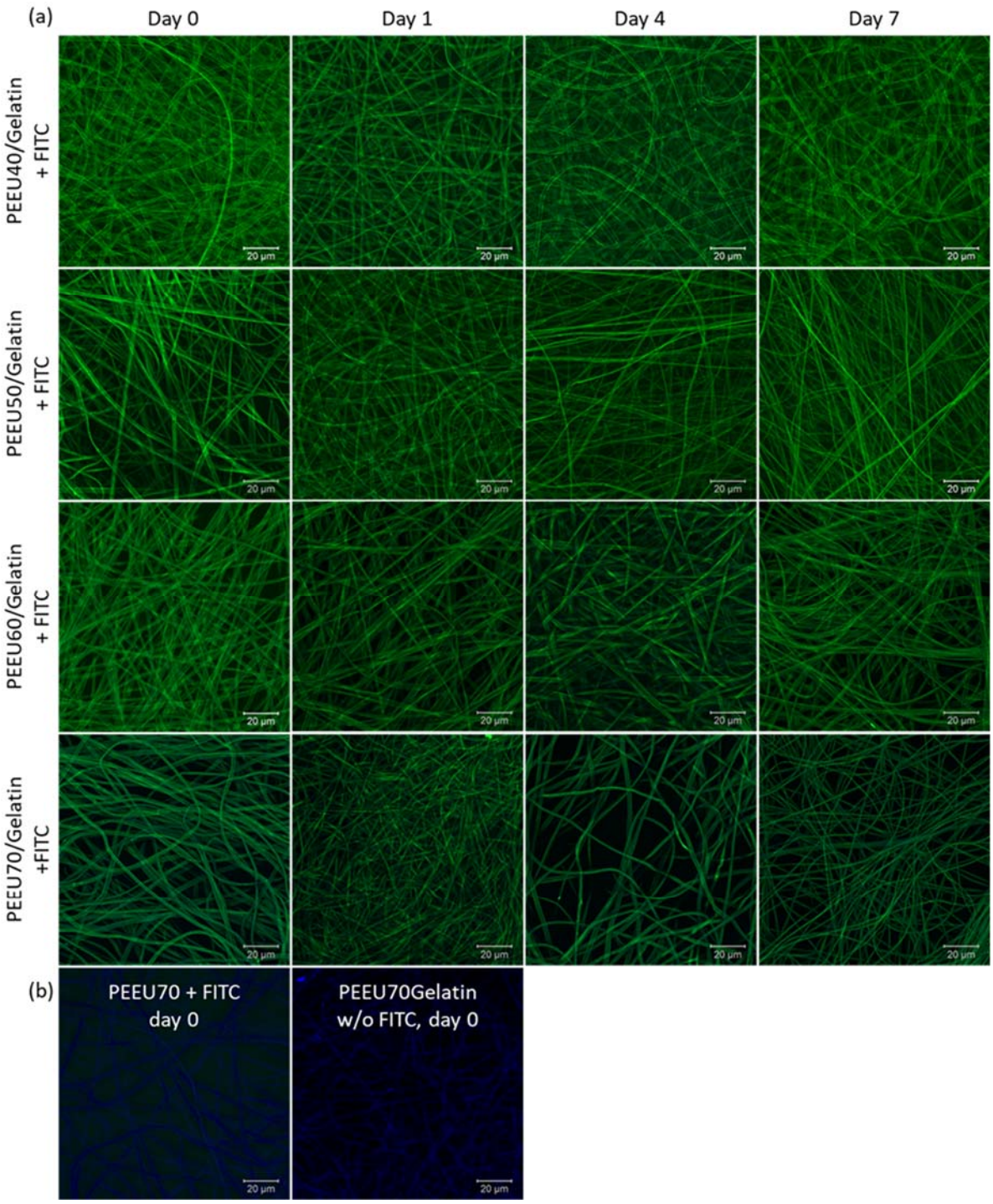

Figure 5. Stability of gelatin on PEEU/Gelatin fibers in an aqueous environment. (a) FITC conjugated PEEU/Gelatin fibers over 7 days in PBS at 37 °C. (b) PEEU70/Gelatin fibers and PEEU70 was used as a control example showing the pure PEEU fibers did not give any green fluorescent signal due to the absence of -NH_2 group for conjugation and PEEU/Gelatin fibers require conjugation of FITC to acquire the green fluorescence signal but not from auto-fluorescence.

Stability of gelatin layer of PEEU/Gelatin fibers

The water solubility of gelatin means that extra chemical reagents are typically required to crosslink the gelatin shell [27,30,35]. In this study, we propose that the gelatin layer could be held on the PEEU surface by molecular entanglement and therefore retained in aqueous environment. The PEEU/Gelatin fibers were conjugated with NHS-FITC for fluorescent determination of gelatin stability on fibers in an aqueous environment. The FITC conjugated PEEU/Gelatin fibers were incubated in PBS at 37 ^{o}C for 7 days before samples were collected in a similar fashion to the parallel hADSC cell culture. From the fluorescent images (Fig. 5a), the gelatin layer of the PEEU fibers was retained over 7 days in a physiological environment, indicating crosslinking was not necessary.

hADSC cell culture on PEEU and PEEU/Gelatin fibers

PEEU/Gelatin fiber meshes showed higher initial cell attachment than for the PEEU fiber meshes. Although the cell seeding density was 1 x 10^4 cells per fiber sample, the low cell seeding efficiency meant that the majority of fiber samples had below 1000 cells attached in the PEEU group, with PEEU50 as an exception (Fig. 6). For the PEEU50 sample, its smaller fiber diameter likely provided a higher surface to volume ratio for cell attachment. On day 7, the PEEU50 had the highest cell number in the PEEU sample group (Fig. 6 and Fig. 7a). However, the observed cell number remained similar to that measured on day 1, indicating no increase in cell number by proliferation. For the other PEEU fiber samples, a low cell attachment was observed at the beginning of culture, when compared to PEEU50, but with a greater increase in cell number over 7 days.

For the PEEU/Gelatin fiber group, certain PEEU/Gelatin fiber meshes were seen to shrink in size immediately after contact with aqueous solution. This shrinking took place as the circumference of the fiber mesh folded toward the center, resulting in a reduced area for cells seeding. PEEU50/Gelatin samples, which had the smallest fiber diameter among the PEEU/Gelatin fiber meshes, showed the highest cell attachment on day 1 within the PEEU/Gelatin group, with a cell number comparable to that of PEEU50. The cell attachment on day 1 for PEEU40/Gelatin and PEEU70/Gelatin fiber samples also showed higher cell numbers when compared to that of the PEEU40 and PEEU70 fiber samples, respectively.

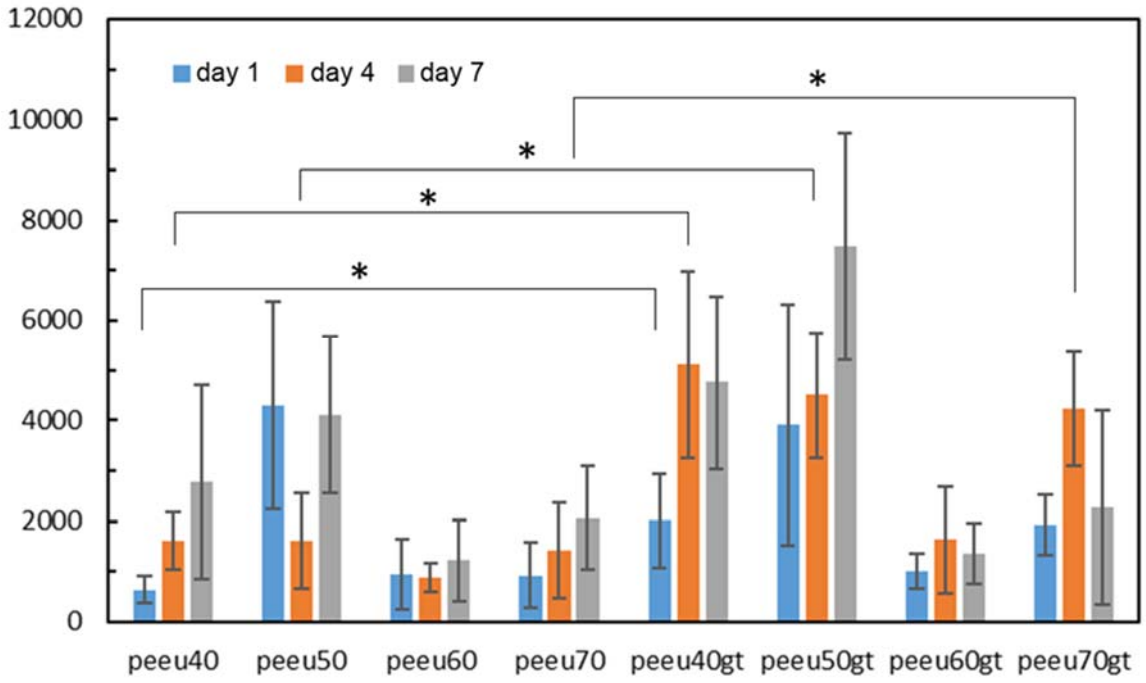

Figure 6. hADSC proliferation on PEEU and PEEU/Gelatin fiber meshes. (n = 4). *: $p < 0.05$. gt: gelatin

Over a 7 day period, PEEU40/Gelatin and PEEU50/Gelatin fiber samples showed an increase in cell number, with PEEU50/Gelatin giving the highest value in the PEEU/Gelatin fiber group (Fig. 6 and Fig. 7b). The cell number on day 7 for the PEEU60/Gelatin and PEEU70/Gelatin samples showed slightly higher cell numbers when compared to PEEU60 and PEEU70 samples, respectively. An increase in cell number of 81.7 ± 34.1% was observed for PEEU50/Gelatin over PEEU50 fiber samples after 7 days of culture. This suggested that the smaller fiber diameter and gelatin layer on the PEEU fibers increased cell attachment and proliferation. The corresponding cell image of PEEU/Gelatin fibers is shown in Fig. 7, demonstrating the higher cell number on PEEU50/Gelatin fibers. Here, the incorporation of a gelatin shell on PEEU polymer fibers enhanced cell attachment and proliferation, an effect that could be further improved by reducing the fiber diameter.

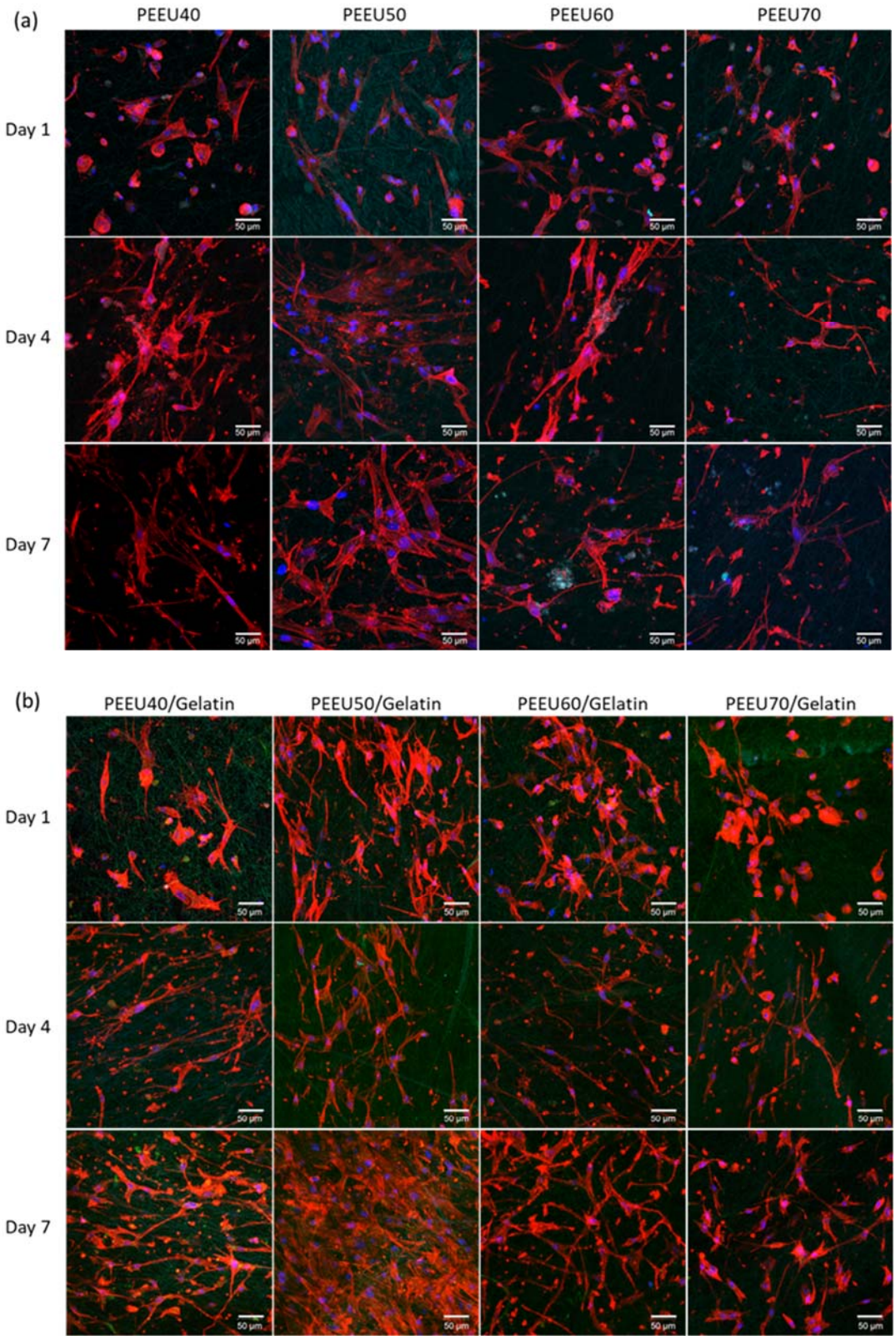

Figure 7. hADSC cell culture on PEEU and PEEU/Gelatin fibers. (a) hADSC on PEEU fibers on day 1, 4, and 7. Red: actin, Blue: nucleus, Cyan: PEEU fiber auto-fluorescent. (b) hADSC on PEEU/Gelatin fibers on day 1, 4 and 7. Red: actin, Blue: nucleus, Green: FITC conjugated gelatin.

Conclusion

A biocompatible interface, necessary to enhance cellular functionality, can be integrated into fibrous scaffolds with high surface to volume ratios. A co-axial electrospinning method, and the use of a unified solvent system for both materials, enabled the deposition of gelatin onto each individual PEEU fiber with molecular entanglement induced fixation. This method avoids the use of cytotoxic crosslinking reagent and any crosslinking induced changes in fiber morphology. With a gelatin shell on the PEEU fibers, a reduction in elastic modulus but increase in elongation at break was observed in water at 37 ^{o}C. The non-crosslinked gelatin shell was found to be stable in an aqueous environment, and enhanced hADSC attachment and proliferation. The co-axial electrospinning method described here, significantly improves on existing cross-linking based methods to produce gelatin coated polymer fiber meshes, and provides insight into the design of core-shell fibrous scaffolds in biomedical research.

Acknowledgements

This work was financially supported by the Helmholtz Association of German Research Centers through program-oriented funding and the Helmholtz Graduate School for Macromolecular Bioscience (MacroBio) with grant no. VH-GS-503 (W. T.).

References

[1] Tibbitt MW, Dahlman JE, Langer R. Emerging Frontiers in Drug Delivery. J Am Chem Soc 2016,138:704–17.

[2] Li J, Mooney DJ. Designing hydrogels for controlled drug delivery. Nat Rev Mater 2016, 1:16071

[3] Maitz MF. Applications of synthetic polymers in clinical medicine. Biosurface Biotribology 2015, 1:161–76.

[4] Mir M, Ali M, Barakullah A, Gulzar A, Arshad M, Fatima S, et al. Synthetic polymeric biomaterials for wound healing: a review. Prog Biomaterials 2018, 7:1–21.

[5] Kamoun EA, Kenawy E-RS, Chen X. A review on polymeric hydrogel membranes for wound dressing applications: PVA-based hydrogel dressings. J Adv Res 2017, 8:217–33.

[6] Teo AJ, Mishra A, Park I, Kim Y-J, Park W-T, Yoon Y-J. Polymeric Biomaterials

for Medical Implants and Devices. Acs Biomater Sci Eng 2016, 2:454–72.
[7] Agarwal R, García AJ. Biomaterial strategies for engineering implants for enhanced osseointegration and bone repair. Adv Drug Deliver Rev 2015, 94:53–62.
[8] Sharma U, Concagh D, Core L, Kuang Y, You C, Pham Q, et al. The development of bioresorbable composite polymeric implants with high mechanical strength. Nat Mater 2017, 17:96.
[9] Theocharis AD, Skandalis SS, Gialeli C, Karamanos NK. Extracellular matrix structure. Adv Drug Deliver Rev 2016, 97:4–27.
[10] Wolf MT, Dearth CL, Sonnenberg SB, Loboa EG, Badylak SF. Naturally derived and synthetic scaffolds for skeletal muscle reconstruction. Adv Drug Deliver Rev 2015, 84:208–21.
[11] Wade RJ, Bassin EJ, Rodell CB, Burdick JA. Protease-degradable electrospun fibrous hydrogels. Nat Commun 2015, 6:6639.
[12] Jiang T, Carbone EJ, Lo K, Laurencin CT. Electrospinning of polymer nanofibers for tissue regeneration. Prog Polym Sci 2015, 46:1–24.
[13] Miguel SP, Figueira DR, Simões D, Ribeiro MP, Coutinho P, Ferreira P, et al. Electrospun polymeric nanofibres as wound dressings: a review. Colloid Surf B-Biointerfaces 2018, 169:60–71.
[14] Cronin-Golomb M, Sahin O. High-resolution nanomechanical analysis of suspended electrospun silk fibers with the torsional harmonic atomic force microscope. Beilstein J Nanotech 2013, 4:243–8.
[15] Perestrelo T, Correia M, Ramalho-Santos J, Wirtz D. Metabolic and Mechanical Cues Regulating Pluripotent Stem Cell Fate. Trends Cell Biol 2018, 28:1014–29.
[16] Menkhaus TJ, Fong H. Chapter 16 Electrospun Nanofibers for Protein Adsorption.In: Electrospinning: Nanofabrication and Applications, ed.: Ding B, Wang X, Yu J, 2019, 517–42.
[17] Liu M, Duan X-P, Li Y-M, Yang D-P, Long Y-Z. Electrospun nanofibers for wound healing. Mater Sci Eng C 2017, 76:1413–23.
[18] Son Y, Kang J, Kim H, Yoo H. Electrospun Nanofibrous Sheets for Selective Cell Capturing in Continuous Flow in Microchannels. Biomacromolecules 2016, 17:1067–74.
[19] Geiger B, Spatz JP, Bershadsky AD. Environmental sensing through focal adhesions. Nat Rev Mol Cell Bio 2009, 10:1
[20] Muncie JM, Weaver VM. The Physical and Biochemical Properties of the

Extracellular Matrix Regulate Cell Fate. Curr Top Dev Biol 2018, 1–37.
[21] Doan TQ, Leslie SL, Kim S, Bhargava R, White SR, Sottos NR. Characterization of core-shell microstructure and self-healing performance of electrospun fiber coatings. Polymer 2016,107:263–72.
[22] Hou L, Zhang X, Mikael PE, Lin L, Dong W, Zheng Y, et al. Biodegradable and Bioactive PCL–PGS Core–Shell Fibers for Tissue Engineering. Acs Omega 2017, 2:6321–8.
[23] Naeimirad M, Zadhoush A, Kotek R, Neisiany R, Khorasani S, Ramakrishna S. Recent advances in core/shell bicomponent fibers and nanofibers: A review. J Appl Polym Sci 2018, 135:46265.
[24] Hu X, Liu S, Zhou G, Huang Y, Xie Z, Jing X. Electrospinning of polymeric nanofibers for drug delivery applications. J Control Release 2014, 185:12–21.
[25] Sohrabi A, Shaibani PM, Etayash H, Kaur K, Thundat T. Sustained drug release and antibacterial activity of ampicillin incorporated poly(methyl methacrylate)–nylon6 core/shell nanofibers. Polymer 2013, 54:2699–705.
[26] Merkle V, Zeng L, Slepian M, Wu X. Core-shell nanofibers: Integrating the bioactivity of gelatin and the mechanical property of polyvinyl alcohol. Biopolymers 2014, 101: 336-46.
[27] Ravichandran R, Venugopal JR, Sundarrajan S, Mukherjee S, Ramakrishna S. Poly(glycerol sebacate)/gelatin core/shell fibrous structure for regeneration of myocardial infarction. Tissue Eng Part A 2011, 17: 1363-73
[28] Tamimi E, Ardila D, Haskett D, Doetschman T, Slepian M, Kellar R, et al. Biomechanical Comparison of Glutaraldehyde-Crosslinked Gelatin Fibrinogen Electrospun Scaffolds to Porcine Coronary Arteries. J Biomechanical Eng 2016, 138:011001.
[29] Baiguera S, Gaudio C, Lucatelli E, Kuevda E, Boieri M, Mazzanti B, et al. Electrospun gelatin scaffolds incorporating rat decellularized brain extracellular matrix for neural tissue engineering. Biomaterials 2014, 35:1205–14.
[30] Zhao P, Jiang H, Pan H, Zhu K, Chen W. Biodegradable fibrous scaffolds composed of gelatin coated poly(ϵ-caprolactone) prepared by coaxial electrospinning. J Biomed Mater Res A 2007, 83:372-382
[31] Hiebl B, Mrowietz C, Goers J, Bahramsoltani M, Plendl J, Kratz K, et al. In vivo evaluation of the angiogenic effects of the multiblock copolymer PDC using the hen's egg chorioallantoic membrane test. Clin Hemorheol Microcirc 2010, 46:233–8.

[32] Kratz K., Habermann, R., Becker, T., Richau, K. & Lendlein, A. Shape-memory properties and degradation behavior of multifunctional electro-spun scaffolds. Int J Artif Organs 34**,** 225–230 (2011).
[33] Topuz F, Uyar T. Electrospinning of gelatin with tunable fiber morphology from round to flat/ribbon. Mater Sci Eng C 2017, 80:371–8.
[34] Koombhongse S, Liu W, Reneker DH. Flat polymer ribbons and other shapes by electrospinning. J Polym Sci Part B Polym Phys 2001, 39:2598–606.
[35] Merkle V, Zeng L, Teng W, Slepian M, Wu X. Gelatin shells strengthen polyvinyl alcohol core–shell nanofibers. Polymer 2013, 54:6003–7.
[36] Lee J, Tae G, Kim Y, Park I, Kim S-H, Kim S. The effect of gelatin incorporation into electrospun poly(l-lactide-co-ε-caprolactone) fibers on mechanical properties and cytocompatibility. Biomaterials 2008, 29:1872–9.